Non-Destructive Classification of Oil Palm Ripeness Using Free-Space Measurement: An Evaluation of the Nicolson-Ross-Weir Method

Yosy Rahmawati
Department of Electrical Engineering, Faculty of Engineering, Universitas Indonesia, Depok, Jawa Barat, Indonesia
yosy.rahmawati@ui.ac.id

Fitri Yuli Zulkifli
Department of Electrical Engineering, Faculty of Engineering, Universitas Indonesia, Depok, Jawa Barat, Indonesia
yuli@eng.ui.ac.id

Mia Rizkinia
Department of Electrical Engineering, Faculty of Engineering, Universitas Indonesia, Depok, Jawa Barat, Indonesia
mia@ui.ac.id (corresponding author)

Received: 6 November 2025 | Revised: 14 January 2026, 6 February 2026, 10 February 2026, and 11 February 2026 | Accepted: 13 February 2026

 DOI: https://doi.org/10.48084/etasr.16060

ABSTRACT

This study presents a non-destructive free-space electromagnetic sensing system for classifying the ripeness of oil palm fruits. Free-Space Measurement (FSM) was performed over a frequency range of 1 to 26 GHz to acquire reflection (S_{11}) and transmission (S_{21}) responses from oil palm fruit at three stages of ripeness: unripe, ripe, and overripe. The Nicolson-Ross-Weir (NRW) formulation was applied as a mathematical transformation tool to extract frequency-dependent electromagnetic response features, rather than to determine intrinsic dielectric material properties. The measured transmission responses exhibit systematic variations with ripeness. Unripe fruit shows a stronger electromagnetic interaction with resonance behavior occurring in lower frequency regions, while ripening leads to a consistent shift of resonance features toward higher frequencies. These trends are associated with physiological changes during maturation, including moisture reduction, oil accumulation, and tissue degradation. This work is an exploratory feasibility study that emphasizes comparative electromagnetic response trends and system-level resonance behavior under fixed measurement conditions, rather than absolute material characterization. The results demonstrate the potential of free-space electromagnetic sensing as a non-contact approach for oil palm ripeness classification and provide preliminary response features to support future development of microwave, Software-Defined Radio (SDR), and Artificial Intelligence (AI)-based precision agriculture sensing systems. This study experimentally demonstrates that dielectric-based inversion using the NRW formulation becomes unstable and non-physical when applied to a free-space Vector Network Analyzer (VNA) configuration involving non-homogeneous oil palm fruit, as evidenced by phase ambiguity and negative extracted parameters.

Keywords-free-space electromagnetic sensing; non-destructive ripeness classification; oil palm fruit; transmission response (S21); NRW-based feature extraction; precision agriculture

I. INTRODUCTION

Oil palm (*Elaeis guineensis*) is one of the most important agricultural commodities in Indonesia, playing a central role in the global vegetable oil industry for both domestic consumption and export [1]. The oil palm sector contributes significantly to income generation, employment, and regional development [2]. Indonesia is among the largest oil palm producers, with a continuous expansion of plantation areas and production capacity [3]. The sustainability and productivity of this industry depend on efficient plantation management, particularly in the accurate determination of fruit ripeness at harvest [4]. The quality of harvested Fresh Fruit Bunches

(FFB) directly affects downstream processing performance, as harvesting fruit at suboptimal ripeness leads to reduced oil yield and inferior oil quality [5, 6].

Therefore, accurate and objective determination of ripeness is essential to ensure processing efficiency, product quality, and long-term industry sustainability [7]. However, ripeness assessment in current plantation practice still relies heavily on conventional visual inspection based on fruit color, the presence of loose fruits, and bunch morphology [8]. These methods are inherently subjective and prone to inconsistency, especially under varying environmental conditions, plantation management practices, and fruit varieties. As a result, there is a need for more reliable, objective, and non-destructive approaches to oil palm ripeness classification that can reduce uncertainty, minimize harvest losses, and support precision agriculture applications.

Non-destructive electromagnetic sensing methods, such as Free-Space Measurement (FSM), have been explored for agricultural and biological sensing applications due to their ability to probe internal structures without physical contact [9]. FSM employs microwave signals to acquire reflection (S_{11}) and transmission (S_{21}) responses, which are sensitive to changes in internal composition such as moisture distribution, tissue structure, and oil content [10]. The non-contact nature of FSM makes it suitable for fragile, irregular, and heterogeneous biological samples, including oil palm fruit. Rather than direct material characterization, FSM-based sensing captures system-level electromagnetic responses that reflect combined interactions between the sample and the measurement configuration.

Ripening-related physiological changes influence microwave responses in fruits, primarily due to variations in moisture content, oil accumulation, and structural degradation [11]. Unripe fruits, which typically contain higher water content, exhibit a stronger electromagnetic interaction, while ripening leads to systematic changes in the transmission and reflection behavior across frequencies [12]. It has been demonstrated that frequency-dependent electromagnetic responses can serve as reliable indicators of fruit ripeness when evaluated comparatively under consistent measurement conditions. However, for non-homogeneous and lossy biological samples, extracted dielectric parameters should be interpreted cautiously, as they may reflect transformed response features rather than intrinsic material properties.

The NRW formulation has been widely used as a mathematical inversion technique to transform measured S-parameters into frequency-dependent electromagnetic response features [13, 14]. In practical FSM configurations involving near-field operation and irregular biological samples, this study employs NRW as a signal transformation tool to enhance sensitivity to ripening-related trends, rather than as a strict metrological method for dielectric characterization. Furthermore, SDR-based radar systems have shown great potential for real-time, non-contact agricultural sensing [15]. Although this work focuses on FSM-based measurements, the extracted electromagnetic response features and observed resonance behavior provide valuable guidance for the future development of SDR-based sensing systems, particularly for precision agriculture applications requiring flexible frequency operation and short measurement distances [16-22].

However, when FSM is applied to non-homogeneous biological objects like whole oil palm fruits, the validity of dielectric-based inversion methods such as NRW becomes questionable. Phase ambiguity, sample thickness variation, and internal structural heterogeneity may lead to inversion instability and non-physically extracted parameters. Therefore, it is important to experimentally evaluate the applicability and limitations of the NRW formulation under realistic FSM-VNA configurations before interpreting the extracted results.

This study proposes a non-destructive oil palm ripeness classification approach based on a free-space electromagnetic sensing system. Rather than performing intrinsic dielectric material characterization, the study focuses on identifying extracted electromagnetic response features that vary systematically with fruit ripeness. Changes in moisture content, oil accumulation, and tissue structure during ripening are reflected in the measured transmission and reflection behavior. The resulting electromagnetic response trends provide preliminary sensing signatures that can support the development of short-range, non-contact sensing systems for practical plantation and post-harvest applications.

Accordingly, this research analyzes the reflection (S_{11}) and transmission (S_{21}) parameters of oil palm fruits at different stages of ripeness using FSM under fixed and repeatable measurement conditions. The measured S-parameters are further processed using the NRW formulation as a mathematical transformation tool to enhance the sensitivity to frequency-dependent response variations rather than to derive absolute dielectric material properties. The analysis aims to identify frequency regions exhibiting the most pronounced and consistent electromagnetic response changes with ripeness, which are relevant for defining operational bands in future SDR-based sensing systems for non-destructive, real-time ripeness assessment.

II. RESEARCH METHODOLOGY

A. State of The Art Methods

Several studies have investigated electromagnetic sensing and FSM techniques for non-contact evaluation of materials and biological samples. In [23], a calibration-free approach used S-parameter data to estimate complex permittivity in multilayer dielectrics, demonstrating the potential of free-space microwave measurements for the analysis of electromagnetic response. In [24], wideband horn antennas were employed for non-contact water-level sensing in plastic pipelines, confirming the effectiveness of free-space configurations for transmission-based electromagnetic sensing. In [25], C-band Synthetic Aperture Radar (SAR) was utilized to estimate soil moisture-related electromagnetic properties, highlighting the suitability of microwave sensing for agricultural monitoring applications.

Microwave-based sensing in heterogeneous and lossy media has been explored. In [26], electromagnetic response variation was investigated in heterogeneous materials using microwave refractometry, while in [27], an electronic sensing technique was developed to assess the quality of used palm oil,

illustrating the applicability of electromagnetic sensing for palm-based materials. These studies underline the adaptability of microwave sensing techniques across engineering and agricultural domains, particularly when interpreted as system-level electromagnetic responses rather than strict material parameters.

In the context of biological materials, a review of dielectric spectroscopy in biological tissues in [28] emphasized the strong correlation between electromagnetic response behavior and moisture content. In [29], FSM was applied to classify oil palm fruit ripeness by analyzing transmission coefficient (S_{21}) variations across maturity stages. The results showed that unripe fruits exhibit lower transmission due to higher moisture content, followed by increased transmission in ripe fruits and a subsequent decrease in overripe stages associated with fatty acid accumulation. Building upon this concept, this study extends free-space electromagnetic sensing by jointly analyzing S_{11} and S_{21} responses and employing a mathematical transformation to identify frequency regions that exhibit consistent ripeness-dependent electromagnetic trends, with the objective of supporting future short-range SDR-based sensing systems.

B. FSM Experimental Setup and Procedure

The experiment employed a free-space electromagnetic sensing configuration to capture ripeness-dependent variations in oil palm fruit response at three maturity stages: unripe, ripe, and overripe. Measurements were conducted using a Rohde & Schwarz ZNA 40 GHz VNA, with Through-Reflect-Line (TRL) calibration applied independently for each antenna configuration. A pair of linearly polarized antennas was arranged in a face-to-face configuration with a fixed separation distance of 67 cm, corresponding to a radiating near-field measurement setup representative of practical short-range sensing scenarios. The measurement system utilized matched transmitting and receiving antenna pairs within their respective operational frequency bands, including log-periodic antennas for 1–18 GHz and horn antennas for 18–26.5 GHz. The far-field distance was estimated using the classical antenna criterion [30]:

$$R_{ff} = \frac{2D^2}{\lambda}$$

where D is the maximum aperture dimension of the antenna and λ is the wavelength corresponding to the lowest operating frequency of the antenna. For the log-periodic antenna operating in the 1–18 GHz band, the maximum aperture dimension is $D = 0.24$ m. At the lowest operating frequency of 1 GHz, the wavelength is $\lambda = 0.3$ m, resulting in an estimated far-field distance of:

$$R_{ff,LP} = \frac{2(0.24)^2}{0.3} \approx 0.38 \text{ m}$$

For the horn antenna operating in the 18–26.5 GHz band, the aperture dimension is $D = 0.022$ m. At the lowest operating frequency of 18 GHz, the wavelength is $\lambda = 0.0167$ m, yielding a far-field distance of:

$$R_{ff,Horn} = \frac{2(0.022)^2}{0.0167} \approx 0.06 \text{ m}$$

In the experimental configuration, the total transmitting–receiving antenna separation was fixed at 67 cm, with the oil palm fruit sample positioned at the midpoint. Consequently, the antenna-to-sample distance was approximately 33.5 cm. Based on the above analysis, the sample is located within the radiating near-field (Fresnel) region for the log-periodic antenna at the lowest frequencies, and well within the far-field region for the horn antenna. Despite satisfying the classical far-field criterion for certain frequency ranges, the measurement configuration does not fulfill the assumptions required for intrinsic dielectric property extraction using the NRW method. This is primarily due to the broadband nature of the antennas, frequency-dependent phase-center variation, and the non-homogeneous structure of the oil palm fruit samples. Therefore, the measured responses are interpreted as system-level electromagnetic sensing signatures rather than intrinsic material properties. Table I summarizes the equipment specifications and system configuration. All measurements were conducted in a semi-anechoic laboratory environment to minimize external electromagnetic interference.

TABLE I. EQUIPMENT SPECIFICATIONS AND CONFIGURATION

Configuration	Specifications
VNA	Rohde & Schwarz ZNA, 40 GHz
Antenna (1–18 GHz band)	Schwarzbeck Mess-Elektronik Log-Periodic Antenna (TX–RX matched pair)
Antenna (18–26.5 GHz band)	Pasternack PE9852-20 Standard Gain Horn Antenna (TX–RX matched pair)
Additional horn antenna	A-INFO MMW Standard Gain Horn Antenna (used for band-specific validation and alignment)
Antenna separation (TX–RX)	67 cm (sample positioned at midpoint)
Antenna-sample sistance	Approximately 33.5 cm
Calibration method	TRL calibration applied independently for each frequency band
Measurement configuration	Free-space transmission–reflection (FSM)
Measurement region	Radiating near-field (1–18 GHz) and far-field (18–26.5 GHz), depending on antenna type
Measurement environment	Semi-anechoic environment

Matched transmitting and receiving antennas were used for each frequency band to avoid bandwidth mismatch and radiation pattern overlap. Whole oil palm fruit bunches with an average diameter of approximately 15 cm were classified into unripe, ripe, and overripe stages based on expert visual assessment. A total of six samples were evaluated, consisting of two samples per stage of ripeness. For each stage, one sample was measured in its original whole-bunch form, while the second sample was manually flattened on the front and back surfaces to approximate a planar measurement interface consistent with FSM and TRL calibration assumptions. Surface flattening was performed to reduce scattering and phase distortion arising from curved geometries, without altering the internal composition of the fruit. All samples were positioned centrally between the transmitting and receiving antennas using a non-metallic holder. The FSM measurement procedure began with air calibration to establish a baseline reference and eliminate system interference. Figure 2 illustrates the experimental setup. After calibration, the reflection (S_{11}) and transmission (S_{21}) parameters were recorded using the VNA.

The measured S-parameters were subsequently processed to extract electromagnetic response features for comparative ripeness analysis.

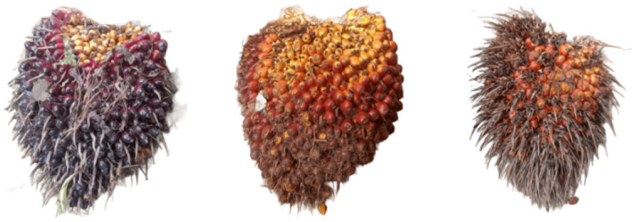

(a) (b) (c)

Fig. 1. Oil palm fruit samples: (a) unripe, (b) ripe, (c) overripe.

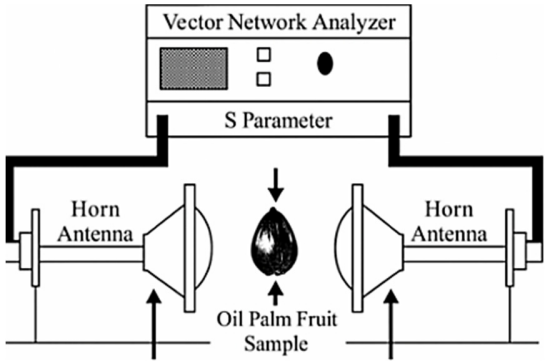

Fig. 2. FSM experimental setup.

C. Data Processing and Electromagnetic Parameter Extraction

Resonance-like frequency behavior in FSM is identified from local minima observed in the transmission parameter S_{21} obtained from VNA measurements. These minima indicate frequency regions where strong interaction occurs between the electromagnetic wave and the fruit under the fixed measurement configuration. Before response extraction, the measured reflection (S_{11}) and transmission (S_{21}) data were processed using a median filter to suppress measurement noise while preserving crucial spectral characteristics. The filtered S-parameter data were subsequently processed using the NRW formulation, which is employed as a mathematical transformation technique to map the measured S-parameters into frequency-dependent electromagnetic response features, rather than as a strict metrological tool for intrinsic material property characterization. The reflection coefficient (Γ) and transmission coefficient (T) were derived from the measured S_{11} and S_{21} parameters, followed by calculation of the complex refractive index (n), which represents phase shift and attenuation effects within the sensing system. Under the non-magnetic assumption ($\mu_r = 1$), the transformed relative permittivity term ($\varepsilon_r = n^2$) is employed as an extracted dielectric response parameter. The real (ε') and imaginary (ε'') components are interpreted as frequency-dependent response features that reflect combined system-sample interactions under near-field and non-ideal measurement conditions, rather than absolute intrinsic material properties. The NRW equations employed in this study are [31-33]:

$$\Gamma = \frac{[(S_{11})^2-(S_{21})^2+1]}{[2 \cdot S_{11}]} \quad (1)$$

$$T = \frac{S_{21}}{(1-\Gamma)} \quad (2)$$

$$n = \left(\frac{c}{(j\omega d)}\right) \times ln\left(\frac{1}{T}\right) \quad (3)$$

$$\varepsilon_r = n^2 \rightarrow (\mu_r = 1) \quad (4)$$

Since the refraction index n is complex, it can be expressed as:

$$n = n' - jn'' \quad (5)$$

which yields a complex extracted effective dielectric response:

$$\varepsilon_r = (n' - jn'') \quad (6)$$

$$\varepsilon' = (n')^2 - (n'')^2 \quad (7)$$

$$\varepsilon'' = 2n'n'' \quad (8)$$

where Γ is the reflection coefficient, T is the transmission coefficient, n is the complex refractive index, ε_r is the extracted dielectric response parameter, ω is the angular frequency (rad/s), and d is the effective propagation length.

In this study, the NRW formulation is intentionally applied under conditions that do not strictly satisfy its underlying assumptions, including non-homogeneous samples, near-field operation, and limited sample repetition. This enables an experimental evaluation of the stability and validity of dielectric-based inversion when applied to FSM-VNA sensing of biological objects. Instability in the extracted parameters, including sign reversal and near-zero magnitudes, is therefore treated as experimental evidence of the NRW limitation rather than a measurement error.

D. Measurement Uncertainty and Experimental Limitations

Free-space electromagnetic sensing of non-homogeneous biological samples is inherently subject to multiple sources of uncertainty, including VNA calibration tolerance, antenna alignment, sample positioning, surface curvature, antenna configuration, and environmental conditions. The FSM system was calibrated using the TRL method, which assumes planar reference interfaces; therefore, deviations from ideal planar surfaces in whole fruit bunches may introduce additional scattering and phase distortion. To mitigate this effect, supplementary measurements were conducted on samples with manually flattened front and back surfaces to better approximate planar measurement conditions consistent with TRL assumptions. Additional uncertainty arises from the use of non-identical antenna types, limited antenna separation, and near-field operation, which may contribute geometry-dependent and antenna-dependent effects to the measured S-parameters.

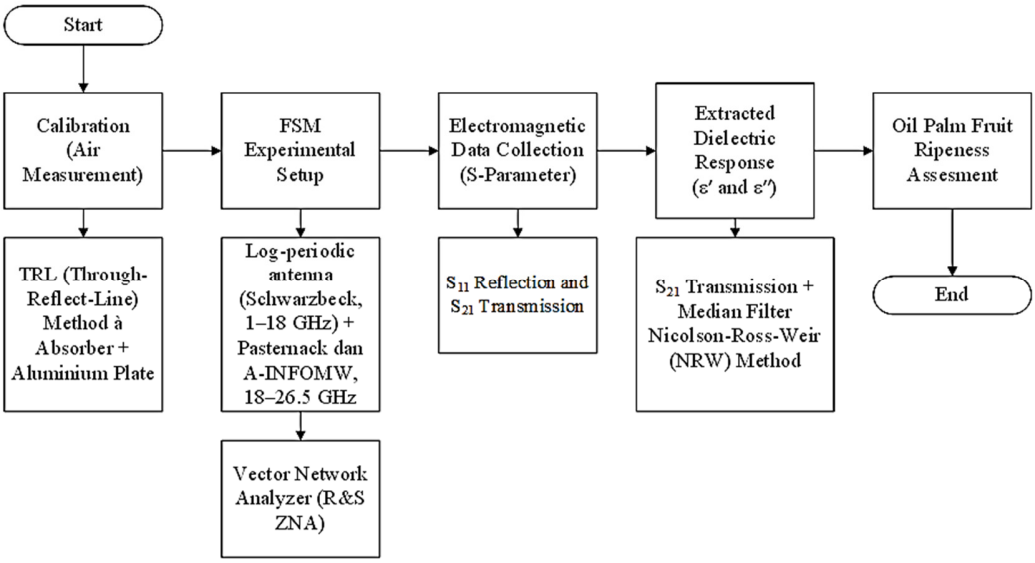

Fig. 3. Measurement procedure.

Due to the exploratory nature of this study and the limited number of samples, formal uncertainty quantification and statistical error analysis were not performed. Consequently, the extracted dielectric response parameters are interpreted as system-level electromagnetic responses obtained under fixed and repeatable experimental conditions. These limitations are explicitly acknowledged and will be addressed in future work through improved antenna symmetry, optimized measurement geometry, repeated measurements, and larger sample sets.

III. EXPERIMENTAL RESULTS AND VERIFICATION

A. FSM Implementation

Oil palm fruit measurements were conducted using the free-space electromagnetic sensing configuration shown in Figure 4, designed to reflect short-range, field-relevant sensing conditions. The system was calibrated using the TRL method with aluminum and absorber standards to establish a consistent reference for S-parameter measurements. Log-periodic antennas (1–18 GHz) and horn antennas (18–26.5 GHz) were used in matched transmitting and receiving pairs, connected to a VNA (Rohde & Schwarz ZNA), to record reflection (S_{11}) and transmission (S_{21}) parameters.

The measured S-parameter data were processed using a median filter to suppress noise while preserving key spectral features. The filtered data were subsequently transformed using the NRW formulation as a mathematical response extraction tool to enhance sensitivity to frequency-dependent electromagnetic variations. Resonance-like behavior was identified from local minima in the S_{21} response. The resulting extracted electromagnetic response features were analyzed comparatively across ripeness stages to evaluate ripeness-dependent trends.

The experimental dataset consists of free-space S-parameter measurements acquired from whole oil palm fruit samples at three ripeness stages: unripe, ripe, and overripe. A total of six samples were evaluated, with two samples per ripeness category. Reflection (S_{11}) and transmission (S_{21}) parameters were measured for each sample over the 1–26 GHz frequency range using a VNA under identical experimental conditions. The measured S-parameter data were processed utilizing a median filter to suppress measurement noise while preserving essential spectral and resonance features. Subsequent analysis focused on frequency-dependent transmission minima, extracted dielectric response trends, and comparative electromagnetic behavior across ripeness stages, rather than on absolute intrinsic material parameter estimation.

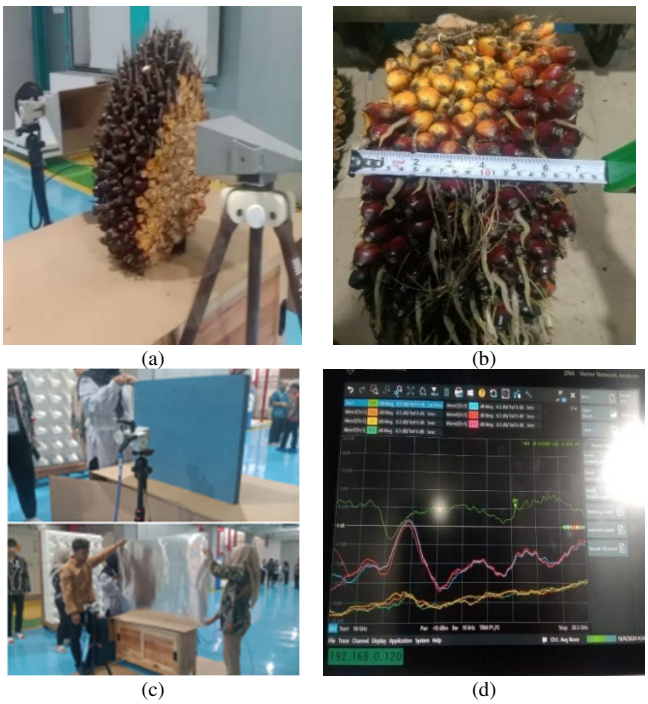

Fig. 4. FSM measurement implementation on oil palm fruit: (a) FSM configuration, (b) sample thickness, (c) TRL calibration, (d) VNA.

B. Characteristics of S_{11} and S_{21} Parameters

The S_{21} transmission response, displayed in Figure 5, exhibits distinct resonance-like minima for each ripeness stage, indicating frequency regions where strong interaction occurs between the incident electromagnetic wave and the fruit under the fixed sensing configuration. A systematic shift of these resonance-like features toward higher frequencies is observed as ripening progresses. This behavior is associated with the combined effects of moisture reduction, oil accumulation, and internal structural changes, supporting the use of S_{21} as an effective, non-destructive electromagnetic sensing indicator for ripeness differentiation.

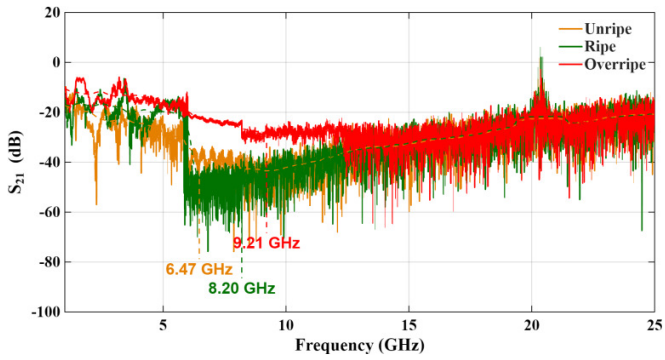

Fig. 5. S_{21} transmission graph.

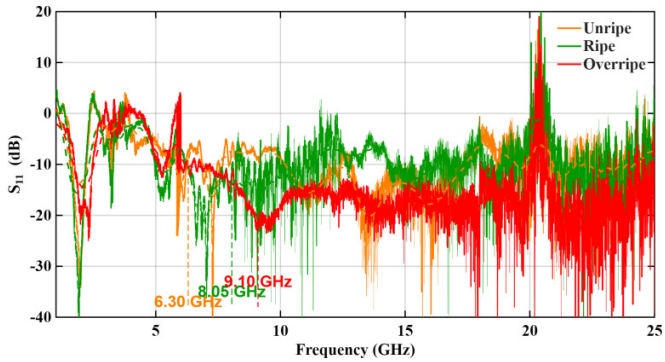

Fig. 6. S_{11} reflection graph.

The S_{11} reflection response, illustrated in Figure 6, represents the portion of the incident wave reflected at the fruit-air interface, providing complementary information on surface and near-surface interaction. Although S_{11} is not used directly to determine resonance-like frequencies, variations in reflection behavior across ripeness stages are consistent with reduced moisture content and increased structural degradation in riper fruit, further supporting the observed transmission trends.

C. Extracted Dielectric Response (ε' and ε'')

Processing the FSM data using the NRW formulation yields an extracted dielectric response, represented by the real (ε') and imaginary (ε'') components derived from the measured S_{11} and S_{21} parameters. Figure 7 presents the frequency-dependent ε' and ε'' responses for different ripeness stages. Systematic variations are observed across ripeness levels.

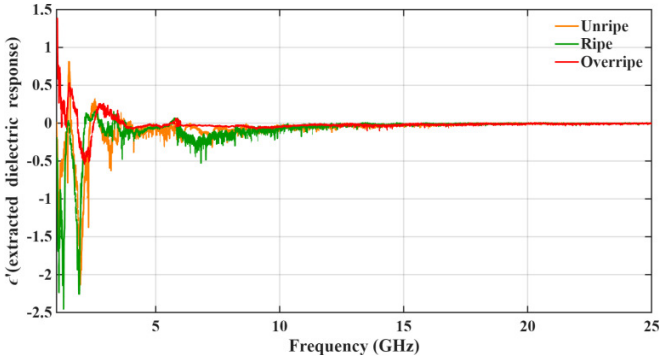

(a)

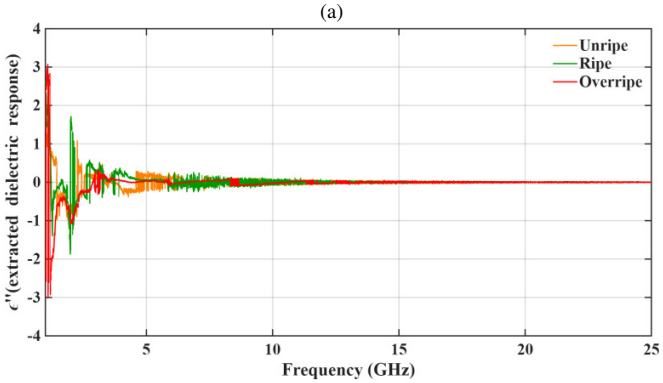

(b)

Fig. 7. Extracted dielectric response of oil palm fruit : (a) real part (ε'), (b) imaginary part (ε'').

D. Experimental Evidence of NRW Inversion Instability

The extracted dielectric response exhibits non-physical characteristics, including negative real components ($\varepsilon' < 0$) and near-zero magnitudes across multiple frequency regions. These behaviors are indicative of phase ambiguity in the logarithmic inversion of the NRW formulation, which becomes highly sensitive to small variations in S_{21} when transmission levels are low. Furthermore, measurements were conducted on a limited number of samples (one representative sample per ripeness stage for NRW extraction). As a result, non-physical inversion results are not statistically averaged out, and their impact becomes pronounced. This experimental observation confirms that dielectric-based inversion using NRW is not valid for absolute material characterization in the FSM-VNA-non-homogeneous fruit configuration.

The occurrence of negative real permittivity (ε') values originates from the mathematical inversion process of the NRW formulation rather than from the physical properties of the oil palm fruit. In this free-space configuration, electromagnetic waves propagate through multiple paths within the non-homogeneous fruit structure, resulting in phase superposition and ambiguity. The logarithmic operation used to extract the complex refractive index becomes multi-valued under these conditions, leading to an incorrect branch selection, and consequently a negative real component of the refractive index. Since ε' is obtained as the square of the refractive index, this phase ambiguity directly results in negative ε' values. In contrast, the imaginary component ε'' remains positive, as it is predominantly governed by transmission magnitude attenuation

S_{21}, which consistently reflects electromagnetic loss within the sample. Therefore, the negative ε' values observed in this study represent non-physical inversion results of the NRW method under non-ideal and non-homogeneous measurement conditions, rather than intrinsic dielectric material properties.

E. Scatter Analysis of Extracted Electromagnetic Response

Figure 8 depicts the scatter distribution of the extracted ε' and ε'' components for unripe, ripe, and overripe oil palm fruit samples.

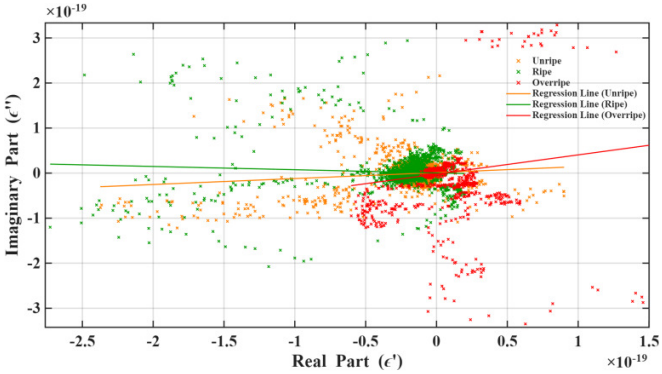

Fig. 8. Correlation between extracted dielectric response (ε_r) and oil palm fruit ripeness.

Distinct clustering patterns are observed for each ripeness stage, indicating different electromagnetic response behaviors under identical measurement conditions. This separation demonstrates the capability of the extracted response features to differentiate ripeness levels in a non-destructive manner. The observed variations are associated with physiological changes during ripening, including moisture loss, oil accumulation, and tissue softening, which influence electromagnetic energy storage and dissipation. Although the extracted parameters do not represent intrinsic material properties, the consistent correlation between electromagnetic response patterns and ripening processes supports their practical use for non-destructive ripeness classification.

F. Correlation Between Extracted Electromagnetic Response and Ripeness

Table II summarizes representative extracted electromagnetic response values (ε' and ε'') observed near resonance-like frequency regions for unripe, ripe, and overripe samples. The reported values reflect relative electromagnetic interaction behavior rather than absolute material parameters. Higher ε'' values observed in unripe fruit indicate stronger electromagnetic energy dissipation associated with higher moisture content. As ripening progresses, reductions in ε'' and changes in ε' reflect diminished electromagnetic interaction due to moisture loss, oil accumulation, and increased internal air gaps. These systematic trends indicate that moisture content is a dominant factor influencing the extracted electromagnetic response during ripening, reinforcing the relevance of the proposed sensing approach.

TABLE II. EXTRACTED NRW-BASED ELECTROMAGNETIC RESPONSE PARAMETERS

Maturity stage	Real part (ε')	Imaginary part (ε'')
Unripe	-0.020835	0.009704
Ripe	-0.060576	0.010386
Overripe	-0.005124	0.002086

The reported ε' and ε'' values are system-dependent electromagnetic response parameters obtained from NRW inversion under non-ideal conditions, and do not represent intrinsic dielectric constants of oil palm fruit.

G. Applicability of the NRW Transformation and Resonance Interpretation

The NRW formulation was originally developed for homogeneous, planar materials under ideal measurement conditions. When applied to whole oil palm fruit bunches, which are non-homogeneous and geometrically irregular, the extracted response is influenced by structural complexity, internal air gaps, surface curvature, and near-field interaction effects. Consequently, resonance-like features observed in the S_{21} response may arise from a combination of dielectric contrast, sample thickness, and geometric resonance effects. For this reason, the observed resonance-like frequencies are interpreted as system-level electromagnetic responses, rather than intrinsic material resonances. Despite these limitations, consistent shifts in resonance-like behavior and extracted electromagnetic response features were observed across ripeness stages under identical sensing configurations, supporting the exploratory feasibility of the proposed free-space electromagnetic sensing approach for comparative, non-destructive ripeness assessment. Therefore, the primary contribution of this work is not dielectric property extraction, but the experimental evaluation of NRW applicability and the identification of robust electromagnetic response trends suitable for non-destructive ripeness classification.

H. Comparison with Previous Studies

The NRW algorithm is widely used as a transformation of S-parameter data, but its physical interpretation becomes less reliable on non-homogeneous samples due to structural complexity and measurement configuration dependencies [34]. Advanced studies have shown that NRW inversion can be unstable and produce non-unique extracted responses under such conditions [35]. In biological and agricultural sensing, microwave techniques extract effective electromagnetic responses that correlate with changes in sample properties, even though these do not represent intrinsic dielectric properties [36]. Accordingly, this study interprets NRW-derived quantities as extracted dielectric responses for comparative ripeness analysis rather than as an intrinsic material constant.

IV. CONCLUSION

This study investigated a free-space electromagnetic sensing system for non-destructive classification of oil palm fruit ripeness using reflection and transmission measurements. The extracted electromagnetic response features and resonance-like behavior exhibited consistent and systematic variations across unripe, ripe, and overripe stages, corresponding to

physiological changes such as moisture reduction, oil accumulation, and tissue degradation during ripening. Due to the non-homogeneous nature of whole fruit bunches and near-field measurement conditions, the transformed response parameters obtained using the Nicolson-Ross-Weir (NRW) formulation are interpreted as system-level electromagnetic responses rather than intrinsic material properties. Despite these limitations, the consistent response trends observed under identical sensing configurations demonstrate the exploratory feasibility of the proposed approach for non-contact ripeness classification. The findings provide preliminary electromagnetic sensing signatures that can support future development of short-range microwave sensing systems, including integration with Software-Defined Radio (SDR) platforms and Artificial Intelligence (AI)-based estimation frameworks for practical precision agriculture applications. This study experimentally confirms that dielectric-based NRW inversion is not valid for intrinsic material characterization of non-homogeneous oil palm fruit under Free-Space Measurement-Vector Network Analyzer (FSM-VNA) configurations, due to phase ambiguity and inversion instability. Nevertheless, the transformed electromagnetic response features remain effective for comparative ripeness classification.

ACKNOWLEDGMENT

This research was supported by Hibah PUTI Q2 under contract number NKB-711/UN2.RST/HKP.05.00/2024 from Universitas Indonesia. The authors also acknowledge financial support from the Indonesian Education Scholarship (Beasiswa Pendidikan Indonesia – BPI), Center for Higher Education Funding and Assessment (PPAPT), and Indonesian Endowment Fund for Education (LPDP), Ministry of Finance of the Republic of Indonesia.

REFERENCES

[1] B. P. Forster *et al.*, "Oil Palm (Elaeis guineensis)," in *Genetic Improvement of Tropical Crops*, H. Campos and P. D. S. Caligari, Eds. Springer International Publishing, 2017, pp. 241–290.

[2] H. Purnomo *et al.*, "Reconciling oil palm economic development and environmental conservation in Indonesia: A value chain dynamic approach," *Forest Policy and Economics*, vol. 111, Feb. 2020, Art. no. 102089, https://doi.org/10.1016/j.forpol.2020.102089.

[3] R. Astuti *et al.*, "Making illegality visible: The governance dilemmas created by visualising illegal palm oil plantations in Central Kalimantan, Indonesia," *Land Use Policy*, vol. 114, Mar. 2022, Art. no. 105942, https://doi.org/10.1016/j.landusepol.2021.105942.

[4] R. Khatun, M. I. H. Reza, M. Moniruzzaman, and Z. Yaakob, "Sustainable oil palm industry: The possibilities," *Renewable and Sustainable Energy Reviews*, vol. 76, pp. 608–619, Sept. 2017, https://doi.org/10.1016/j.rser.2017.03.077.

[5] Z. B. M. Sharif, N. B. M. Taib, M. S. B. Yusof, M. Z. B. Rahim, A. L. B. M. Tobi, and M. S. B. Othman, "Study on Handing Process and Quality Degradation of Oil Palm Fresh Fruit Bunches (FFB)," *IOP Conference Series: Materials Science and Engineering*, vol. 203, May 2017, Art. no. 012027, https://doi.org/10.1088/1757-899X/203/1/012027.

[6] A. A. Kader and D. M. Barrett, "Classification, Composition of Fruits, and Postharvest Maintenance of Quality," in *Processing Fruits: Science and Technology*, CRC Press, 1996, pp. 1–24.

[7] N. J. Lam *et al.*, "Classification of banana stages using microwave spectroscopy by machine learning," *Tạp chí Khoa học Đại học Đồng Tháp*, vol. 14, no. 04S, pp. 174–188, Mar. 2025, https://doi.org/10.52714/dthu.14.04S.2025.1577.

[8] N. Khan, M. A. Kamaruddin, U. U. Sheikh, Y. Yusup, and M. P. Bakht, "Oil Palm and Machine Learning: Reviewing One Decade of Ideas, Innovations, Applications, and Gaps," *Agriculture*, vol. 11, no. 9, Aug. 2021, Art. no. 832, https://doi.org/10.3390/agriculture11090832.

[9] C. Origlia, D. O. Rodriguez-Duarte, J. A. T. Vasquez, J. C. Bolomey, and F. Vipiana, "Review of Microwave Near-Field Sensing and Imaging Devices in Medical Applications," *Sensors*, vol. 24, no. 14, July 2024, https://doi.org/10.3390/s24144515.

[10] C. Y. Beinga, N. Hashima, B. Maringgala, and M. H. Wondic, "A review of non-destructive techniques applied for measuring quality of oil palm fresh fruit bunches," *Journal of Agricultural and Food Engineering*, vol. 1, no. 1, pp. 1–6, Mar. 2020, https://doi.org/10.37865/jafe.2020.0002.

[11] N. Alsmairat, Y. Othman, J. Ayad, M. Al-Ajlouni, J. Sawwan, and N. El-Assi, "Anatomical Assessment of Skin Separation in Date Palm (Phoenix dactylifera L. var. Mejhoul) Fruit during Maturation and Ripening Stages," *Agriculture*, vol. 13, no. 1, Dec. 2022, Art. no. 38, https://doi.org/10.3390/agriculture13010038.

[12] J. Y. Goh, Y. Md Yunos, and M. S. Mohamed Ali, "Fresh Fruit Bunch Ripeness Classification Methods: A Review," *Food and Bioprocess Technology*, vol. 18, no. 1, pp. 183–206, Jan. 2025, https://doi.org/10.1007/s11947-024-03483-0.

[13] S. Sahin, N. K. Nahar, and K. Sertel, "A Simplified Nicolson–Ross–Weir Method for Material Characterization Using Single-Port Measurements," *IEEE Transactions on Terahertz Science and Technology*, vol. 10, no. 4, pp. 404–410, July 2020, https://doi.org/10.1109/TTHZ.2020.2980442.

[14] F. Costa, M. Borgese, M. Degiorgi, and A. Monorchio, "Electromagnetic Characterisation of Materials by Using Transmission/Reflection (T/R) Devices," *Electronics*, vol. 6, no. 4, Nov. 2017, Art. no. 95, https://doi.org/10.3390/electronics6040095.

[15] S. Oncu, "Perfomance Assessment of Real Time Radar Classification on Software-Defined Radio (SDR) Platforms," M.S. Thesis, Gazi University, Turkey, 2024.

[16] F. Niaz, J. Zhang, M. Khalid, M. Younas, and A. Niaz, "mmFruit: A Contactless and Non-Destructive Approach for Fine-Grained Fruit Moisture Sensing Using Millimeter-Wave Technology," *IEEE Transactions on Mobile Computing*, vol. 24, no. 5, pp. 4022–4039, May 2025, https://doi.org/10.1109/TMC.2024.3520914.

[17] Y. K. Kwag, J. S. Jung, I. S. Woo, and M. S. Park, "Modern Software Defined Radar (SDR) Technology and Its Trends," *Journal of electromagnetic engineering and science*, vol. 14, no. 4, pp. 321–328, Dec. 2014, https://doi.org/10.5515/JKIEES.2014.14.4.321.

[18] F. A. F. A. S. de Carvalho, "Implementation of a RADAR system on a software defined radio platform," M.S. Thesis, Universidade de Coimbra, Portugal, 2018.

[19] A. Y. Khaled, S. Abd Aziz, S. K. Bejo, N. Mat Nawi, and I. Abu Seman, "Artificial intelligence for spectral classification to identify the basal stem rot disease in oil palm using dielectric spectroscopy measurements," *Tropical Plant Pathology*, vol. 47, no. 1, pp. 140–151, Feb. 2022, https://doi.org/10.1007/s40858-021-00445-1.

[20] A. Ndiaye, T. Kondengar, M. Ba, E. G. Gbetie, and S. Ouya, "Modernization of Guinean Agriculture through SDR and IoT for Enhanced Connectivity and Monitoring in Rural Areas," in *2024 International Conference on Intelligent Computing and Next Generation Networks (ICNGN)*, Nov. 2024, pp. 1–5, https://doi.org/10.1109/ICNGN63705.2024.10871729.

[21] A. Aghababaei, F. Aghababaei, M. Pignitter, and M. Hadidi, "Artificial Intelligence in Agro-Food Systems: From Farm to Fork," *Foods*, vol. 14, no. 3, Jan. 2025, Art. no. 411, https://doi.org/10.3390/foods14030411.

[22] E. T. Michailidis, K. Maliatsos, and D. Vouyioukas, "Software-Defined Radio Deployments in UAV-Driven Applications: A Comprehensive Review," *IEEE Open Journal of Vehicular Technology*, vol. 5, pp. 1545–1586, 2024, https://doi.org/10.1109/OJVT.2024.3477937.

[23] M. C. Ho and T. H. Le, "Accurate Estimation without Calibration of the Complex Relative Permittivity of Multilayer Dielectric Material based

on the Finite Integration Technique," *Engineering, Technology & Applied Science Research*, vol. 13, no. 3, pp. 10664–10669, June 2023, https://doi.org/10.48084/etasr.5665.

[24] Z. Farid, Z. Najam, M. Y. A. Khan, S. Ahmed, and S. Akhtar, "Perspectives of Water Level Measurement in Plastic Pipes Using Wideband Horn Antenna," *Engineering, Technology & Applied Science Research*, vol. 8, no. 6, pp. 3624–3630, Dec. 2018, https://doi.org/10.48084/etasr.2425.

[25] B. Q. Shakir, M. A. Shareef, and Q. A. M. Al Nuaimy, "Determination of Soil Properties Utilizing C-Band Synthetic Aperture Radar (SAR) in Southern Kirkuk Governate, Northern Iraq," *Engineering, Technology & Applied Science Research*, vol. 15, no. 4, pp. 25407–25416, Aug. 2025, https://doi.org/10.48084/etasr.12189.

[26] S. Shekhar, F. J. Trujillo, S. Kaur, and K. Prasad, "Elucidation of Electrical Characteristics for Apples (Malus domestica) Using Electrochemical Impedance Spectroscopy," *NDT*, vol. 3, no. 4, Oct. 2025, Art. no. 25, https://doi.org/10.3390/ndt3040025.

[27] L. Anifah, P. R. Wikandari, P. W. Rusimamto, . Haryanto, and P. D. Widayaka, "A New Approach to the Quality Determination of Used Palm Cooking Oil using Supervised Learning based on Electronic Sensors," *Engineering, Technology & Applied Science Research*, vol. 14, no. 6, pp. 18171–18177, Dec. 2024, https://doi.org/10.48084/etasr.8913.

[28] D. El Khaled, N. Castellano, J. Gázquez, A. J. Perea-Moreno, and F. Manzano-Agugliaro, "Dielectric Spectroscopy in Biomaterials: Agrophysics," *Materials*, vol. 9, no. 5, Apr. 2016, Art. no. 310, https://doi.org/10.3390/ma9050310.

[29] Y. Rahmawati, M. Rizkinia, and F. Y. Zulkifli, "Palm Fruit Ripeness Characteristics Specification Using Free Space Measurement Method," in *2023 International Conference on Radar, Antenna, Microwave, Electronics, and Telecommunications (ICRAMET)*, Nov. 2023, pp. 386–389, https://doi.org/10.1109/ICRAMET60171.2023.10366605.

[30] C. A. Balanis, *Antenna Theory: Analysis and Design*. John Wiley & Sons, 2016.

[31] S. Boll, "Suppression of acoustic noise in speech using spectral subtraction," *IEEE Transactions on Acoustics, Speech, and Signal Processing*, vol. 27, no. 2, pp. 113–120, Apr. 1979, https://doi.org/10.1109/TASSP.1979.1163209.

[32] A. M. Nicolson and G. F. Ross, "Measurement of the Intrinsic Properties of Materials by Time-Domain Techniques," *IEEE Transactions on Instrumentation and Measurement*, vol. 19, no. 4, pp. 377–382, Nov. 1970, https://doi.org/10.1109/TIM.1970.4313932.

[33] W. B. Weir, "Automatic measurement of complex dielectric constant and permeability at microwave frequencies," *Proceedings of the IEEE*, vol. 62, no. 1, pp. 33–36, 1974, https://doi.org/10.1109/PROC.1974.9382.

[34] J. Baker-Jarvis, M. D. Janezic, J. H. J. Grosvenor, and R. G. Geyer, "Transmission/reflection and short-circuit line methods for measuring permittivity and permeability," National Institute of Standards and Technology (U.S.), NIST Technical Note 1355-R, Dec. 1993.

[35] D. M. Pozar, Microwave Engineering, International Adaptation. John Wiley & Sons, 2021.

[36] S. Gabriel, R. W. Lau, and C. Gabriel, "The dielectric properties of biological tissues: III. Parametric models for the dielectric spectrum of tissues," *Physics in Medicine & Biology*, vol. 41, no. 11, Aug. 1996, Art. no. 2271, https://doi.org/10.1088/0031-9155/41/11/003.